

Positive Ground Flashes Produced by Low-Precipitation Thunderstorms in Oklahoma on 26 April 1984

E. BRIAN CURRAN* AND W. DAVID RUST

NOAA/ERL/National Severe Storms Laboratory, Norman, Oklahoma

(Manuscript received 14 January 1991, in final form 13 August 1991)

ABSTRACT

A group of thunderstorms developed in western Oklahoma during the afternoon of 26 April 1984. Two of these storms initially exhibited characteristics of low-precipitation (LP) thunderstorms. Lightning ground flashes produced by these storms were mostly positive. These storms split, with one right-moving component evolving into a tornadic supercell. Ground flashes produced by the supercell, however, were predominantly negative. The highest rate of positive ground flashes (1.5 min^{-1}) occurred during LP storm splitting and merging, when about 84% of ground flashes were positive. The maximum total ground-strike rate was 3.4 min^{-1} and occurred during the tornadic supercell phase and when all but one of 136 ground flashes were negative. Analysis of lightning ground-strike and radar reflectivity data reveals a concentration of positive ground flashes in areas of maximum reflectivity within the LP storms; furthermore, the concentration of positive flashes appeared during storm split. After storm splitting and merging, the number of positive ground flashes in all cells decreased. Recent studies suggested a relationship between high values of wind-shear magnitude within the cloud-bearing layer and the production of positive ground flashes. Analyses of soundings in the environments of the LP and supercell thunderstorms on this day show that the magnitude of the vector-averaged shear vector within the cloud-bearing layer was 4.8×10^{-3} and $3.8 \times 10^{-3} \text{ s}^{-1}$, respectively. Both are above the previously published thresholds hypothesized for positive flash production. Thus, our analysis suggests that strong shear may be a necessary, but not sufficient, condition for the production of positive ground flashes. Contrary to earlier reports in the literature, our data indicate the height of the -10°C isotherm is not a key parameter for positive flash production in warm-season convection. Finally, a link between positive ground flashes and hail is again suggested.

1. Introduction

Lightning flashes whose return strokes lower positive charge from the cloud to the ground, as opposed to the more frequent negative charge, have been documented in severe thunderstorms and hypothesized to be related to thunderstorm severity (Rust et al. 1981; Reap and MacGorman 1989). From studies of winter thunderstorms in Japan, Takeuti et al. (1978) and Brook et al. (1982) proposed a relationship between the magnitude of wind shear within the cloud-bearing layer and the production of positive ground flashes. They suggested that tilting the thunderstorm dipole down-shear with height facilitates the production of positive ground flashes. Brook et al. (1982) observed that shallow, wintertime convective storms in strongly baroclinic environments produced mostly positive ground flashes. They found an apparent threshold in wind-shear magnitude of $1.5 \times 10^{-3} \text{ s}^{-1}$, above which the

percentage of ground flashes that were positive increased linearly. Rust et al. (1985), in a study of positive ground flashes from tornadic thunderstorms in Oklahoma and Texas, found that storms in an environment where shear magnitudes in the 850–300-mb layer were $>2 \times 10^{-3} \text{ s}^{-1}$ produced mainly positive flashes. One storm moved into an environment possessing a shear magnitude $<2 \times 10^{-3} \text{ s}^{-1}$ in the same layer; the majority of ground flashes then became negative. They also suggested a possible relationship between shear and positive ground flashes. Takeuti et al. (1985) observed a predominance of positive ground flashes in storms in Norway characterized by shear magnitudes $>1 \times 10^{-3} \text{ s}^{-1}$. Since only one of four storms was similar to those in their earlier studies in Japan, they proposed that an additional cause, a significantly lowered height of the -10°C isotherm, is related to positive ground flashes in Norway. Takagi et al. (1986) combined their two-dimensional model of positive lightning initiation with charge densities for convective storms in the literature. The model results support their hypothesis that both vertical wind shear and the height of the charge involved in the lightning directly affect the percentage of ground flashes that are positive. Based on regression analyses of numerical model fields, Reap and MacGorman (1989) found an apparent lack of correlation between large values of

* Present affiliation: National Weather Service, Oklahoma City, OK 73159.

Corresponding author address: Dr. W. David Rust, National Severe Storms Laboratory, Storm Electricity & Cloud Physics Research Group, 1313 Halley Circle, Norman, OK 73069.

wind shear and positive lightning production; thus, the role of shear in the production of positive ground flashes remains questionable. They did report, however, that thunderstorms with large hail can be prolific producers of positive ground flashes.

Reported here are observations of thunderstorms in Oklahoma on 26 April 1984 whose ground flashes were about 60% positive before the tornadic supercell phase. We found it was low-precipitation (LP) storms (Bluestein and Parks 1983) that produced mostly positive ground flashes. One LP storm moved away from the group and evolved into a supercell (Browning 1964); nearly all ground flashes produced by this supercell were negative in polarity.

First, we briefly summarize published studies concerning LP thunderstorms. Ground-flash rates relative to storm evolution will be presented, and positive ground-flash locations relative to the storms' horizontal reflectivity structures will be discussed. Using soundings taken in the LP and supercell storm environments on 26 April 1984, we will address wind shear within the cloud-bearing layer and the height of the -10°C isotherm relative to the production of positive ground flashes by both the LP and supercell thunderstorms.

2. The low-precipitation thunderstorm

Donaldson et al. (1965), Davies-Jones et al. (1976), and Burgess and Davies-Jones (1979) described a unique type of thunderstorm that produces little precipitation at the surface, yet produces large hail. Tornadoes were observed in all three studies. The visual structure of these thunderstorms is also unique in that they consist of a single, bell-shaped cumuliform tower and large anvil (Fig. 1). Striations may be seen along the surface of the cloud, giving the visual manifestation of cloud rotation. The investigators proposed that this type of thunderstorm has a singular intense updraft with no evidence of an accompanying downdraft.

In an extensive photographic and climatological study, Bluestein and Parks (1983) noted the following features as common to these storms:

- 1) proximity to a dryline
- 2) little, if any, precipitation reaches the surface
- 3) evidence of strong updrafts at the storm's rear with no indication of a downdraft at the surface
- 4) large hail falling from outside the main cumuliform tower
- 5) weak to moderate tornadoes

They performed a statistical analysis of various thermodynamic and wind-related parameters associated with documented LP and supercell storms in the southern Plains. From their analysis, they proposed that the environment of the LP storm is generally drier than that of the supercell storm. Furthermore, both the mean tropospheric wind speed and the tropospheric shear magnitude were weaker in the LP storm environments than in the supercell environments. The LP storm, the authors argued, is a type of supercell with low precipitation efficiency.

Weisman and Bluestein (1985) employed a three-dimensional cloud model (Klemp and Wilhelmson 1978) in an attempt to simulate an LP storm by, in effect, turning off the rain process within the model. Precipitation was not allowed to fall to the surface; consequently, there was no development of an evaporatively cooled outflow at the surface. Because of the evidence from numerical simulations, they reasoned that minor differences in the environments of LP and supercell thunderstorms could not explain the precipitation inefficiency of the LP storm. They proposed that higher concentrations of cloud condensation nuclei originating from the drier continental air behind the dryline could limit the drop-size spectrum within the cloud, thus decreasing precipitation efficiency. They also noted that a narrow drop-size spectrum could be

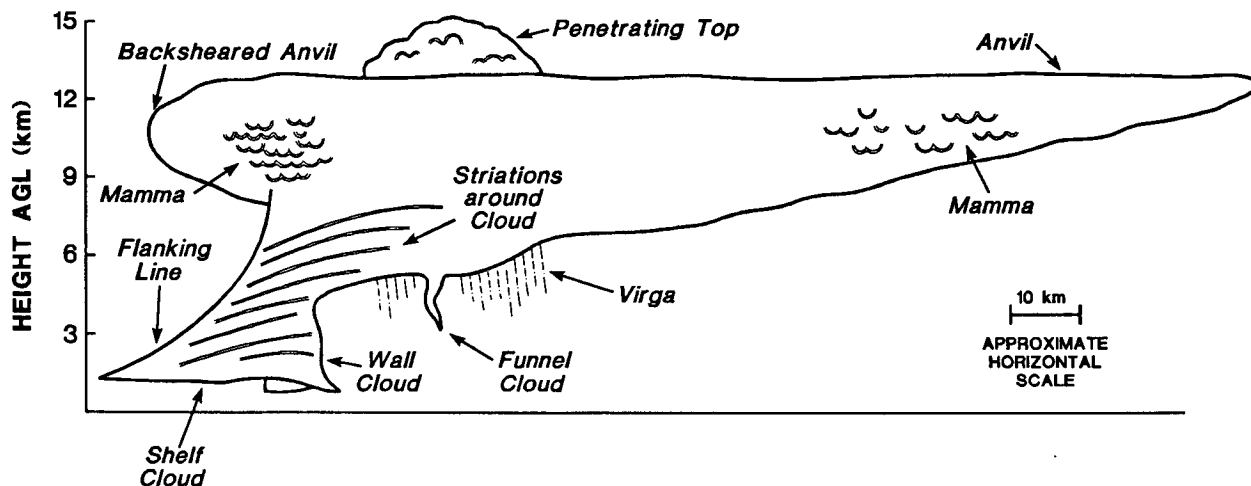


FIG. 1. Schematic of an LP thunderstorm (adapted from Bluestein and Parks 1983).

realized through the growth of the storm from a single isolated cloud. Entrainment of drier ambient air into the cloud also may serve to reduce precipitation efficiency in LP thunderstorms. Unfortunately, no in situ measurements of cloud microphysics within LP thunderstorms have been reported to test their hypotheses.

3. Storm history

a. Meteorological situation

The surface features on the afternoon of 26 April 1984 were typical of those that often produce severe weather outbreaks over the southern Plains. At 2100 (all times UTC), a dryline (Schaefer 1974) extended north through south across Oklahoma (Fig. 2). Thunderstorms formed in west-central Oklahoma about 2200 in response to afternoon heating along the dryline (Burgess and Curran 1985) and moved northeastward (Fig. 3). Cells B and C split into left- and right-moving components (relative to the mean wind), with cell C_L merging with cell B_R. Cell C_R evolved into a supercell and began to produce the first of three tornadoes (F0 and F1 in intensity) at 2353 (U.S. Department of Commerce 1984). A decrease in mixing along the dryline, coupled with an approaching short-wave trough (Fig. 4), resulted in a westward movement of the dryline. By 0000, the dryline had retreated to western Oklahoma, with a low pressure center at the intersection of the dryline and cold front in southwestern Oklahoma (Fig. 5). Cell C_R maintained supercell characteristics until 0238. The other thunderstorms, however, decreased in intensity by 0030. Movement of the short-wave trough over the Plains, deepening of

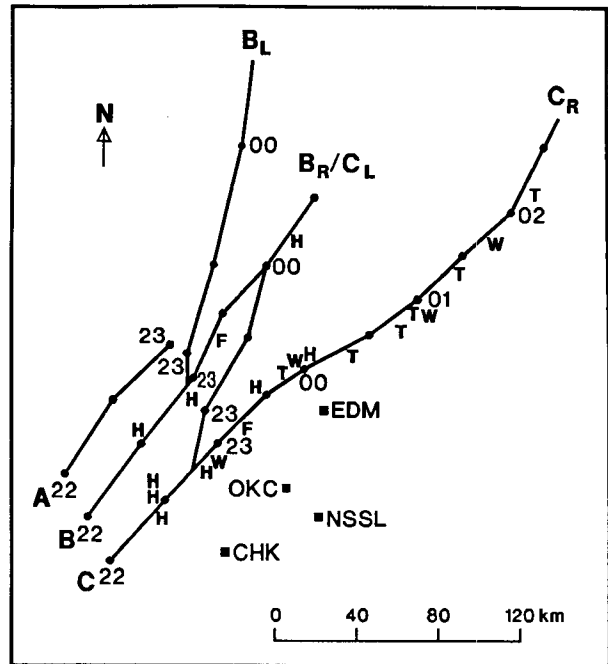


FIG. 3. Echo centroid positions of afternoon thunderstorms on 26 April 1984 taken from the NSSL WSR-57 radar. The letters A, B, and C indicate parent cells, and subscripts L and R correspond to left- and right-moving components, respectively. Severe weather events (H = hail, W = winds, F = funnel, T = tornado) are indicated along cell paths. Time in hours (e.g., 22 = 2200 UTC) and intervening half hours (unlabeled dots along cell paths) are given. Rawinsonde sites at Chickasha (CHK), Edmond (EDM), and Oklahoma City (OKC) are indicated.

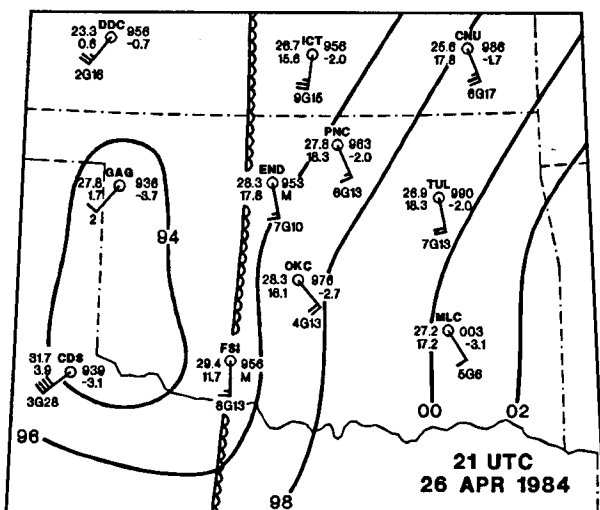


FIG. 2. Surface map at 2100 UTC on 26 April 1984. Contours of altimeter pressure (mb) are given with leading 9 or 10 omitted. Stations are plotted with standard convention with the addition of 3-h altimeter changes just below station altimeter value. Full wind barb is 10 m s⁻¹; half barb is 5 m s⁻¹.

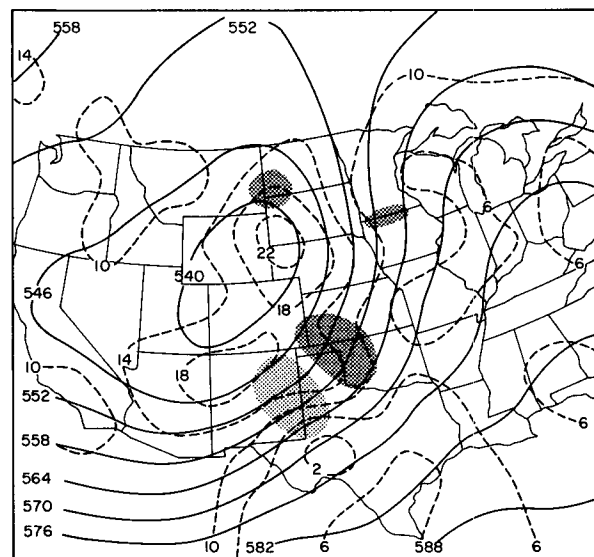


FIG. 4. 500-mb objective analysis for 0000 UTC 27 April 1984. Solid lines indicate heights in dekameters. Dashed lines are relative vorticity isopleths in units of 10⁻⁵ s⁻¹. Dark (light) shading indicates 700-mb rising (sinking) motion in excess of 3 μb s⁻¹. Analysis is a Cressman type with grid spacing of 190 km (after Burgess and Curran 1985).

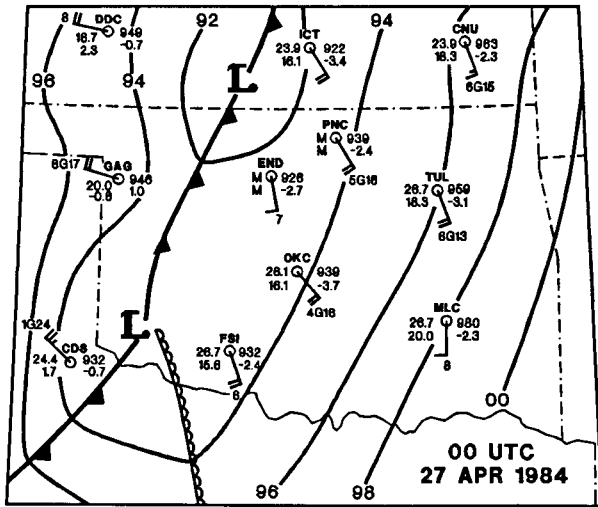


FIG. 5. Surface map at 0000 UTC 27 April 1984, as in Fig. 2.

the surface low in north-central Oklahoma, and strong pressure rises in western Oklahoma served to accelerate the cold front eastward into central portions of the state by 0300 (Fig. 6).

b. 26 April 1984 LP thunderstorm observations

Bluestein and Woodall (1990, hereafter referred to as BW) reported on many aspects of the LP storms of 26 April 1984. We summarize pertinent information from their study and add our observations. Cells B and C initially exhibited characteristics of LP thunderstorms; it is unknown whether cell A also possessed attributes of an LP storm. Large (2-cm) hail fell from cell C at 2227 near Binger, 80 km west of the National Severe Storms Laboratory (NSSL), at 2235 near Hinton (cell B, 85 km west-northwest of NSSL), and 7-cm hail fell at 2258 near Calumet (cell C_L, 70 km northwest of NSSL). A funnel and 2-cm hail were observed by an NSSL intercept team at approximately 2320 near Hennessey (cell B_R, 104 km northwest of NSSL). Photographs taken of these storms do not show an opaque precipitation core. Furthermore, analysis of raingage data indicates a narrow swath (10 km wide) of precipitation amounts mostly <7 mm. The BW study stated that a relatively low concentration of large precipitation particles yielding low precipitation rates may be responsible for the high radar reflectivities (>50 dBZ) and lack of significant light attenuation observed under the cloud base. During its LP phase, cell C passed near NSSL's Stationary Automated Mesonet. The BW study suggested that the existence of a strong, storm-scale gust front was unlikely at 2236. The mesonet measurements of temperature, wet-bulb temperature, pressure, and wind do not show evaporatively cooled outflow air.

Bluestein and Woodall (1990) performed a dual-Doppler radar analysis at 2236 and found that updrafts existed on the northern and southern flanks of cell C, while a downdraft aloft was collocated with the reflectivity core. Both the updrafts and the downdraft were narrower (2–3 km in diameter) and were comparatively weaker aloft (above 6 km) than those found in mature supercells.

c. Ground-flash polarity and rates relative to storm evolution

Lightning ground-flash location and polarity data were collected by the NSSL lightning strike detection network, which has a detection efficiency for negative flashes of about 70% (Mach et al. 1986). The NSSL network has not had its detection efficiency determined for positive ground flashes. Hojo et al. (1989) reported detection efficiencies for their Lightning Location and Protection, Inc. (LLP) network in Japan of 76% for negative and 69% for positive ground flashes in summer. Since their network detection of negative ground flashes is about the same as ours, the detection of positive ground flashes by ours is likely similar. Furthermore, MacGorman and Taylor (1989) analyzed the NSSL network to test the validity of positive ground-flash detection. They concluded that false detection is negligible for flashes with ≥50 LLP amplitude units and <15% for flashes with <50 amplitude units. (These units are arbitrary values for the peak magnetic field radiation normalized to a range of 100 km. They are used in all the LLP ground-strike location systems, e.g., see Orville et al. 1987; Hojo et al. 1989.) In our study, 9 of 42 positive ground flashes from 2202 to 2252 had >50 units. From 2252 to 0037, however, 181 of 192 had >50 units. From an analysis of wave forms identified as positive ground strikes by the SUNYA (State

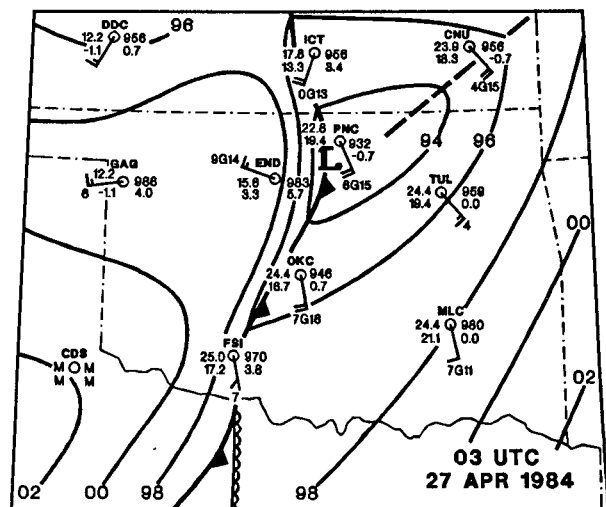


FIG. 6. Surface map at 0300 UTC 27 April 1984, as in Fig. 2.

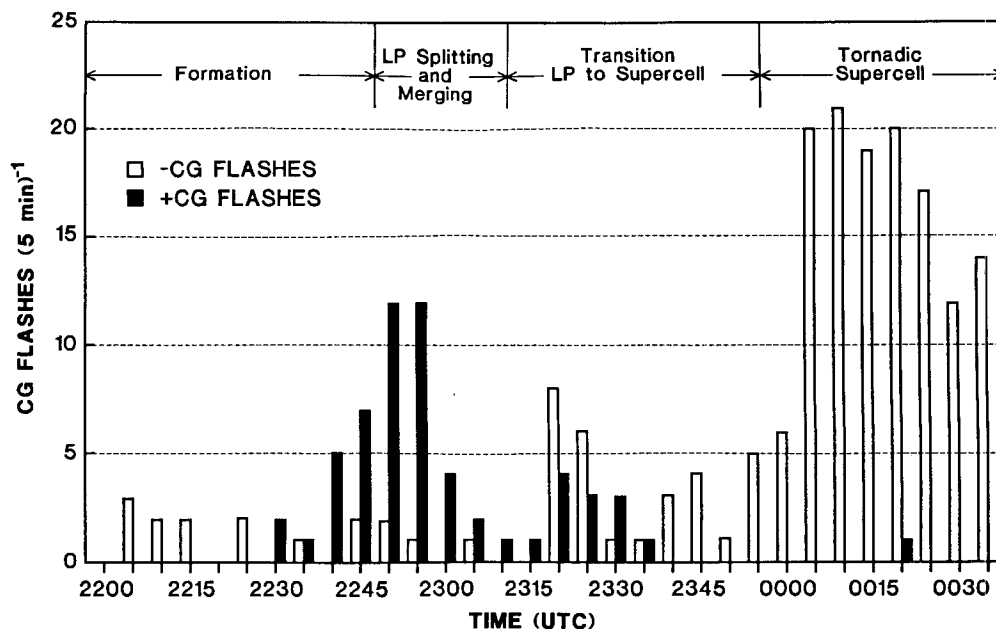


FIG. 7. Lightning ground flashes associated with thunderstorms in Oklahoma on 26 April 1984, in 5-min intervals. Dark bars indicate positive ground flashes; clear bars indicate negative ground flashes. Storm phases are labeled.

University of New York at Albany) detection system, Brook et al. (1989) concluded that positive polarity identification is correct if the flashes are within 600 km of the sensors. Since the flashes were well within 600 km of the NSSL network, there is good evidence that the positive flashes were identified correctly. Thus, false detections are apparently not a factor in our conclusions.

Woodall and Bluestein (1988) defined four phases in the life history of these thunderstorms:

2155–2245: initial formation of thunderstorms and LP severe storms,

2245–2310: LP storm splitting and merging,

2310–2353: transition of LP storm into supercell, and

2353–0238: tornadic supercell thunderstorm.

We sorted the ground-strike data to coincide with these four phases of storm evolution (Fig. 7). During the formation and LP severe-storm phase, lightning ground-flash rates were low, averaging about 0.6 min^{-1} . The number of positive ground flashes increased dramatically during the storm-splitting and storm-merging phase. Thirty-eight of 44 ground flashes during this phase were positive, with a total ground-flash rate of about 1.8 min^{-1} . During the transition phase from LP to supercell thunderstorm, 12 positive and 24 negative ground flashes were observed, with a total ground-flash rate of approximately 1 min^{-1} . Storm intercept observers (Bluestein and Woodall 1990) reported frequent thunder emanating from the storm anvil; ground

flashes, however, were not observed. The average ground-flash rate increased to 3.4 min^{-1} during the tornadic supercell phase of the storm evolution. Positive ground-flash activity was virtually nonexistent during this final phase; only 1 of 136 ground flashes was positive.

4. Ground-flash locations during LP splitting and merging

a. Method

During the storm-splitting and storm-merging phase of LP thunderstorm evolution, 84% of the flashes to ground were positive. We analyzed lightning strike locations relative to the horizontal reflectivity structures during this phase. Because dual-Doppler data were not available from 2240 to 2320, single-Doppler radar data from the NSSL 10-cm wavelength radar in Norman were used to synthesize constant-altitude plan-position indicator (CAPPI) plots. Three volume scans, taken approximately 15 min apart during the splitting and merging phase, were employed. To construct the CAPPIs, a three-dimensional Cressman scheme (Cressman 1959) with horizontal and vertical radii of influence of 1.5 km was used. For each CAPPI, reflectivity data were adjusted to account for storm motion during the volume scan. Lightning ground-flash positions and polarities were then superimposed upon the CAPPIs using a 15-min window centered on the time of each CAPPI. The flash positions were also adjusted to account for storm motion.

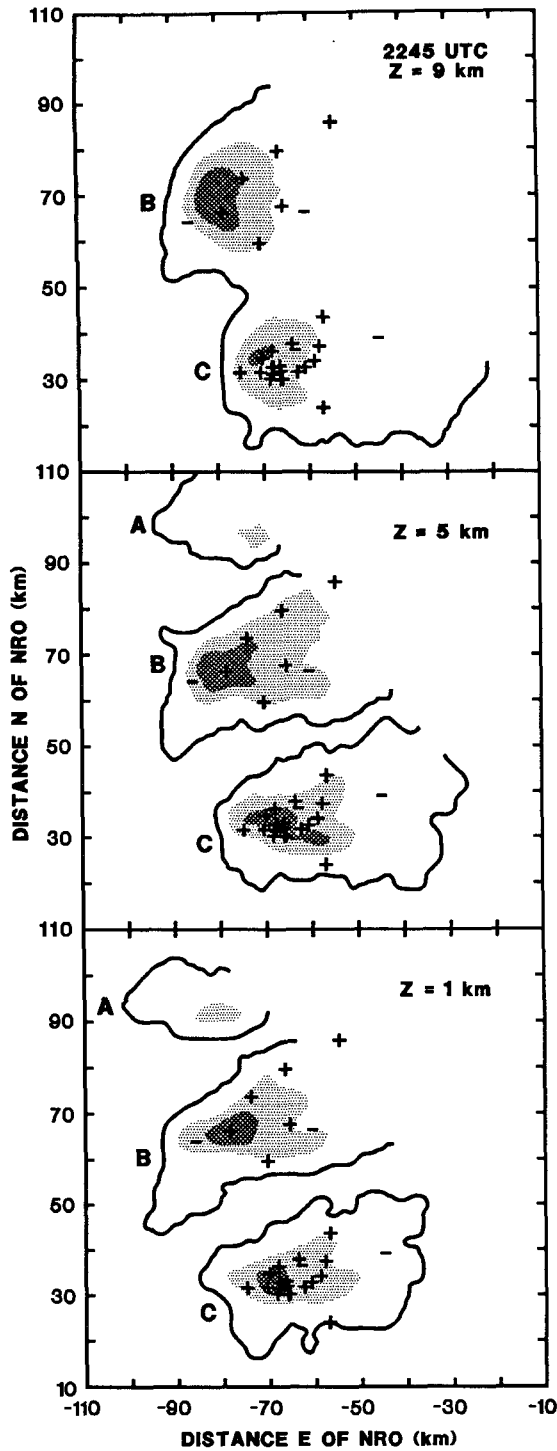


FIG. 8. CAPPs of radar reflectivity at 2245 UTC. Solid line is contour of 10-dBZ reflectivity; striking indicates areas of reflectivity >30 dBZ and hatching >50 dBZ, respectively. Pluses (+) and minuses (-) indicate locations of positive and negative ground flashes, respectively. Letters A, B, and C represent cells designated in Fig. 3. The variable Z is the height (AGL) of each CAPPi. Distances are relative to the NSSL Norman Doppler radar (NRO).

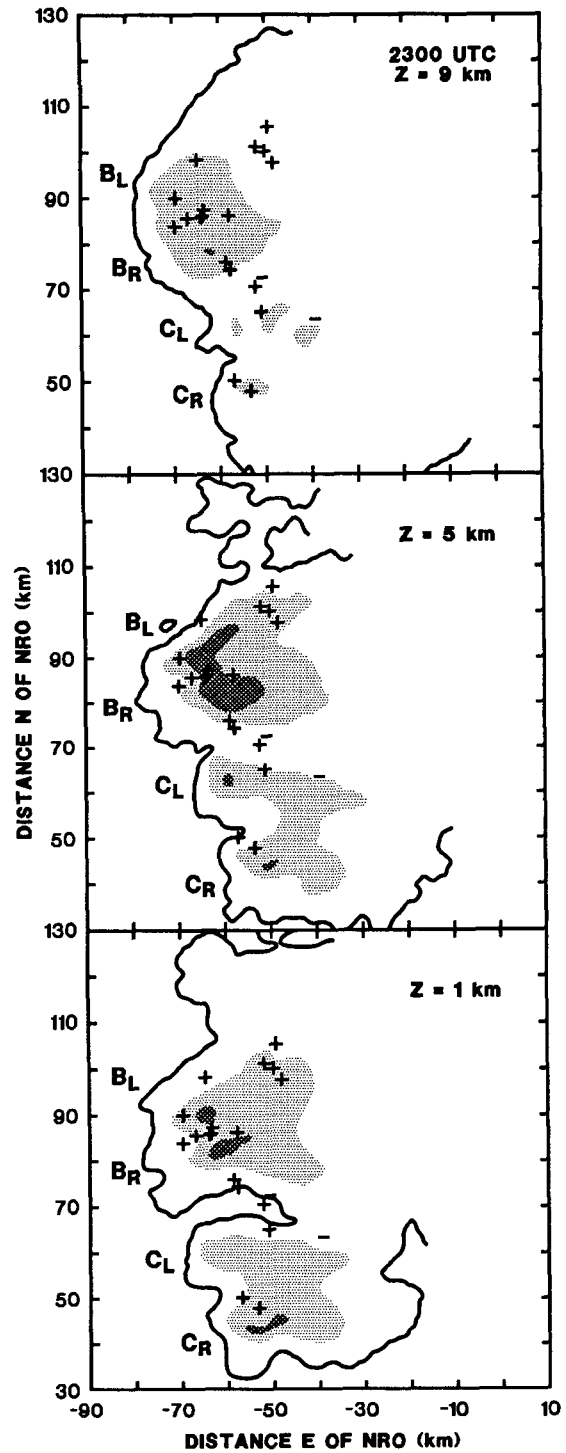


FIG. 9. CAPPs of radar reflectivity at 2300 UTC as in Fig. 8. Subscripts L and R refer to left- and right-moving components as in Fig. 3.

b. Discussion

At 2245 (Fig. 8) cell C was beginning to split aloft. High reflectivities (>50 dBZ) extended to 9 km in both cells B and C. The lightning ground-flash data show a concentration of positive flashes in the reflectivity core (≥ 30 dBZ) of cell C. Positive ground flashes were also occurring in cell B; however, concentration of these flashes is not evident. By 2300 (Fig. 9), cell C split into left- and right-moving components, and cell B was beginning to split. The lightning ground-flash position data show most positive flashes were concentrated in the core of cell B. The number of positive flashes in cell B was less than the number that had occurred in cell C 15 min earlier. In addition, a qualitative decrease in areal extent and intensity of the reflectivity cores aloft is observed in both cells. By 2315 (Fig. 10), cell B had split into left- and right-moving components, with cell B_R merging with cell C_L . Positive flashes to ground were observed within cells B_L and B_R . The reflectivity cores continued to diminish in size and weaken.

The radar reflectivity and ground-strike location analyses show the following: 1) positive ground flashes were concentrated in the reflectivity cores of cells B and C; 2) the spatial concentration of positive ground flashes occurred during storm split; 3) during the storm-splitting phase, the intensity and areal extent of the reflectivity cores diminished; and 4) after both cells B and C split, the number and areal coverage of positive ground flashes decreased.

5. Analysis of thunderstorm proximity soundings

Thirteen rawinsondes were flown on this day from three NSSL sites and from the National Weather Service Forecast Office in Oklahoma City. At 2156, a sounding was taken at the Chickasha site (CHK in Fig. 3). At that time, the afternoon thunderstorms were forming about 60 km west-southwest of CHK. A sounding was made at the Edmond site (EDM in Fig. 3) at 0023, when the tornadic supercell was approximately 30 km north of EDM. Since the soundings were in close spatial and temporal proximity to the LP and supercell storms, we consider them representative of the respective storm environments. The CHK sounding and hodograph are shown in Fig. 11, and the EDM sounding and hodograph are shown in Fig. 12.

We used the thermodynamic and wind data from the CHK and EDM soundings to compute various stability and wind-related parameters in each sounding. Selected values from the sounding analyses are listed in Table 1. The sounding analyses indicate little difference in the thermodynamic characteristics of the environments of the LP and supercell storms. The environment of the supercell storm was slightly drier than the LP storm environment, as evidenced by lower values of precipitable water, contrary to results presented

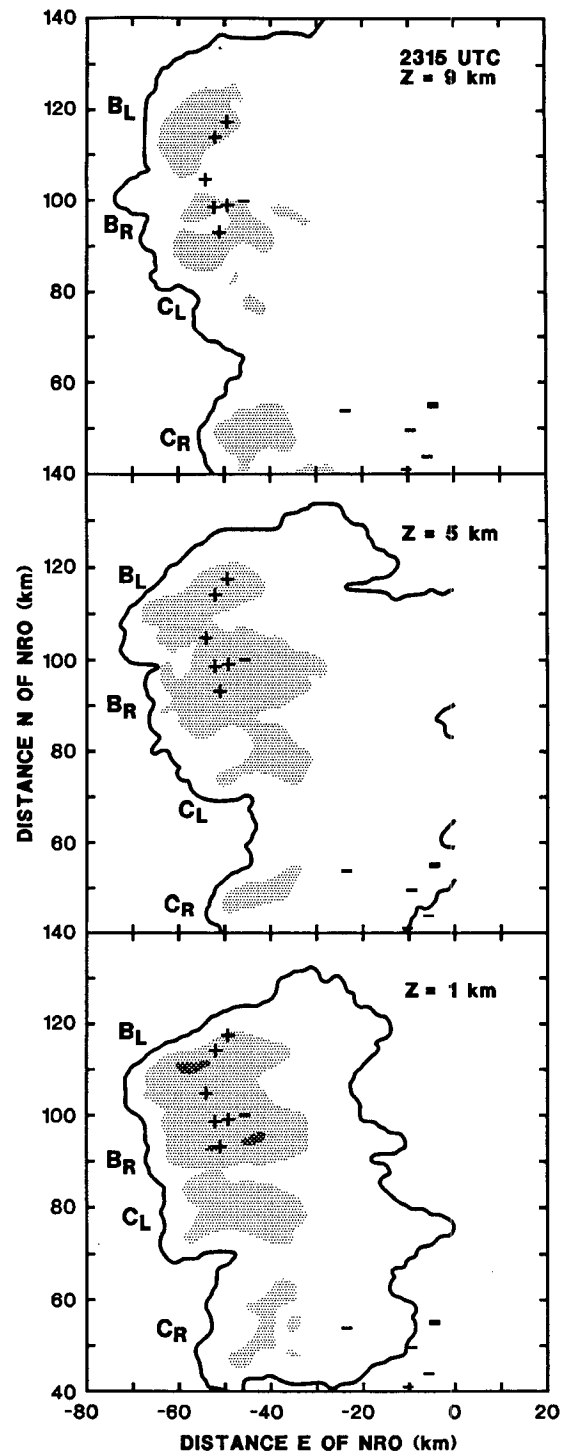


FIG. 10. CAPPIs of radar reflectivity at 2315 UTC, as in Fig. 8.

by Bluestein and Parks (1983). In addition, the lifted index was greater and the convective available potential energy (CAPE) was less in the supercell environment than in the LP environment. Note that the heights of the -10°C isotherm were nearly identical.

The most notable differences between the environments of the LP and supercell thunderstorms, however, are in the wind profiles. The CHK hodograph shows that the winds were generally unidirectional with height. Numerical simulations of convection (Klemp and Wilhelmson 1978; Wilhelmson and Klemp 1978; Schlesinger 1980) demonstrated that storm splitting occurs in model environments characterized by unidirectional winds with height. The EDM hodograph, however, shows clockwise curvature in the lower levels; such an environment favors a right-moving storm with a cyclonically rotating updraft (Weisman and Klemp 1984). Thus, the CHK hodograph would favor splitting storms, while the EDM hodograph would favor a right-moving storm. Both of these phenomena were observed.

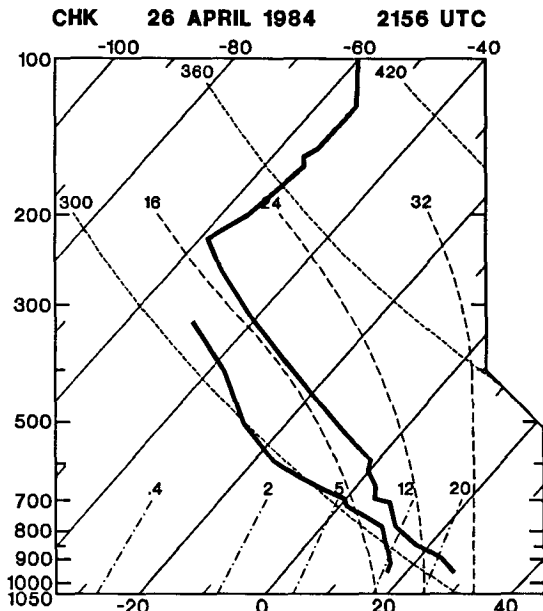


FIG. 11. Skew T -log p (top) and hodograph (bottom) of the CHK sounding at 2156 UTC. Sounding is plotted with normal convention. Hodograph units are in meters per second with numerals on hodograph curve representing heights in kilometers (AGL). The letters L and R denote storm motion for left- and right-moving storms, respectively.

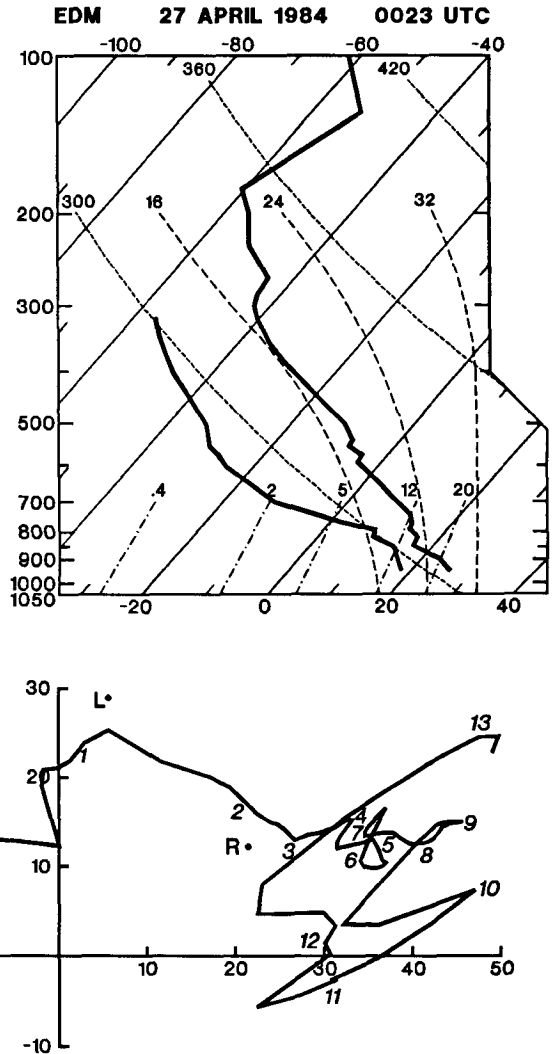


FIG. 12. Skew T -log p (top) and hodograph (bottom) of the EDM sounding at 0023 UTC, as in Fig. 11.

We compare the shear-vector magnitudes on this day with the threshold values in storms with mostly positive ground flashes reported by Brook et al. (1982), Rust et al. (1985), and Takeuti et al. (1985). Brook et al. (1982) calculated the wind shear as the difference in wind speed at the top (from radar) and cloud base (from a sounding) divided by the depth of the cloud. Takeuti et al. (1985) used the 850-mb level and the 500-mb level (approximately cloud top) to derive the depth over which they calculated shear. Rust et al. (1982) used the 850-mb and 300-mb levels similarly, but did a vector calculation to get the magnitude of the shear. Though not identical, the shears are comparable for assessing whether there is a threshold of wind shear within the cloud-bearing layer that affects the production of positive ground flashes.

In their analysis of shear in LP storms, Bluestein and Parks (1983) employed two different calculations:

TABLE 1. Values of thermodynamic and wind parameters from the CHK sounding (Fig. 11) at 2156 UTC 26 April 1984 and the EDM sounding (Fig. 12) at 0023 UTC 27 April 1984.

| Parameter | CHK | EDM |
|--|--------|--------|
| Lifted index ($^{\circ}\text{C}$) | -5.5 | -4.8 |
| Precipitable water (cm) | 3.1 | 2.5 |
| Boundary-layer CAPE (J kg^{-1}) | 2830 | 2261 |
| Height of -10°C isotherm (m MSL) | 5388 | 5415 |
| Cloud-bearing (LCL to EL) mean wind vector (deg/m s^{-1}) | 232/32 | 247/34 |
| Cloud-bearing (LCL to EL) shear vector (deg/m s^{-1}) | 263/48 | 308/38 |
| Cloud-bearing (LCL to EL) magnitude of vector-averaged shear vector (10^{-3} s^{-1}) | 4.8 | 3.8 |

the pressure-weighted magnitude of the vector-averaged shear, and the pressure-weighted scalar-averaged shear magnitude. Their difference is shown through the following example using a circular hodograph of radius 10 m s^{-1} that turns uniformly from 0 to 10 km in height. The magnitude of the vector-averaged shear vector is zero, while the scalar-averaged shear magnitude is $2\pi \times 10^{-3} \text{ s}^{-1}$. Bluestein and Parks (1983) stated that it is not clear which is more informative. Since the magnitude of the vector-averaged shear vector cannot be larger than the scalar-averaged shear magnitude, we use it for a conservative assessment of shear.

To calculate the magnitude of the vector-averaged shear vector, we integrated winds throughout the depth of the cloud. We defined the bottom and top of the cloud to be the lifting condensation level (LCL) and the equilibrium level (EL), respectively. We find that the magnitude of the vector-averaged shear vector within the cloud-bearing layer from the CHK sounding ($4.8 \times 10^{-3} \text{ s}^{-1}$) is greater than the threshold values of 1.5×10^{-3} , 2×10^{-3} , and $3.0 \times 10^{-3} \text{ s}^{-1}$, as reported by Brook et al. (1982), Rust et al. (1985), and Takeuti et al. (1985), respectively. The magnitude of the vector-averaged shear vector within the cloud-bearing layer from the EDM sounding ($3.8 \times 10^{-3} \text{ s}^{-1}$) is also greater than the threshold values.

6. Summary and concluding remarks

Most of the flashes to ground associated with the LP thunderstorms in Oklahoma on 26 April 1984 were positive in polarity. During storm splitting and merging, a peak occurred in the number of positive flashes to ground. Furthermore, the positive ground flashes were concentrated in regions of higher reflectivity. After storm split, one component cell evolved into a supercell. All but one ground flash produced by this storm were negative, with flash rates comparable to those reported by MacGorman et al. (1989) for a supercell storm. Analyses of soundings taken in the environments of the LP and supercell storms show that the values of the magnitude of the vector-averaged shear

vector within the cloud-bearing layer were above previously published threshold values for positive ground-flash production. Thus, a threshold for the magnitude of the vector-averaged shear vector within the cloud-bearing layer may be a necessary, but not sufficient, condition for the production of positive ground flashes. Furthermore, our data do not support the hypothesis that the occurrence of a high percentage of positive ground flashes requires a low-altitude, -10°C isotherm. Our results support the contention by Reap and MacGorman (1989) that positive ground flashes are associated with large hail.

We know of five other LP storms (based on video observations) for which we have ground-flash data. All five LP storms produced mostly positive ground flashes; unfortunately, inadequate radar and rawinsonde data do not merit detailed analysis. This analysis of LP storms on 26 April 1984, along with the other five similar storms, raises several questions:

- 1) Is the predominance of positive ground flashes we observed in LP storms an isolated or a general occurrence?
- 2) Is there a quantitative relationship between large hail and the production of positive ground flashes?
- 3) Do microphysical characteristics that promote precipitation inefficiency in LP thunderstorms significantly influence charge generation and separation within LP storms?
- 4) Is the spatial concentration of positive ground flashes in areas of maximum reflectivity during the LP thunderstorm split related in some way to charge separation?
- 5) Are positive ground flashes associated with splitting or a particular, for example, early stage of a storm's life in a strongly sheared environment?
- 6) What specific role does shear have in the production of positive ground flashes?
- 7) Is the predominance of positive ground flashes in LP storms caused by the same processes that produce more positive than negative ground flashes in the early stage of some non-LP tornadic storms?

Acknowledgments. We thank Donald Burgess, Charles Doswell III, and Robert Davies-Jones for helpful discussions. Donald MacGorman provided the ground-strike data. Glen Anderson and James McGowen operated the NSSL Norman Doppler radar. Kevin Thomas and Kurt Nielsen assisted in processing the Doppler radar and lightning data, respectively. Joan Kimpel drafted the figures.

REFERENCES

- Bluestein, H. B., and C. R. Parks, 1983: A synoptic and photographic climatology of low-precipitation severe thunderstorms in the Southern Plains. *Mon. Wea. Rev.*, **111**, 2034–2046.
- , and G. R. Woodall, 1990: Doppler radar analysis of a low-precipitation thunderstorm. *Mon. Wea. Rev.*, **118**, 1640–1664.

- Brook, M., N. Nakano, P. Krehbiel, and T. Takeuti, 1982: The electrical structure of the Hokuriku winter thunderstorms. *J. Geophys. Res.*, **87**, 1207–1215.
- , R. W. Henderson, and R. B. Pyle, 1989: Positive lightning strokes to ground. *J. Geophys. Res.*, **94**, 13 295–13 303.
- Browning, K. A., 1964: Airflow and precipitation trajectories within severe local storms which travel to the right of the winds. *J. Atmos. Sci.*, **21**, 634–668.
- Burgess, D. W., and R. P. Davies-Jones, 1979: Unusual tornadic storms in eastern Oklahoma on 5 December 1975. *Mon. Wea. Rev.*, **107**, 451–457.
- , and E. B. Curran, 1985: The relationship of storm type to environment in Oklahoma on 26 April 1984. Preprints, *14th Conf. Severe Local Storms*, Indianapolis, Amer. Meteor. Soc., 208–211.
- Cressman, G. P., 1959: An operational objective analysis system. *Mon. Wea. Rev.*, **87**, 367–374.
- Davies-Jones, R. P., D. W. Burgess, and L. R. Lemon, 1976: An atypical tornado-producing cumulonimbus. *Weather*, **31**, 336–347.
- Donaldson, R., A. Spatola, and K. Browning, 1965: Visual observations of severe weather phenomena. *A family outbreak of severe local storms—A comprehensive study of the storms in Oklahoma on 26 May 1963. Part I*. K. A. Browning, Ed., Air Force Cambridge Research Lab., Special Rep. No. 32, 73–97. [AFGL, Hanscom AFB, MA 01731.]
- Hojo, J., M. Ishii, T. Kawamura, F. Suzuki, H. Komuro, and M. Shiogama, 1989: Seasonal variation of cloud-to-ground lightning flash characteristics in the coastal area of the Sea of Japan. *J. Geophys. Res.*, **94**, 13 207–13 212.
- Klemp, J. B., and R. B. Wilhelmson, 1978: The simulation of three-dimensional convective storm dynamics. *J. Atmos. Sci.*, **35**, 1070–1096.
- Lemon, L. R., and C. A. Doswell III, 1979: Severe thunderstorm evolution and mesocyclone structure as related to tornadogenesis. *Mon. Wea. Rev.*, **107**, 1184–1197.
- MacGorman, D. R., and W. L. Taylor, 1989: Positive cloud-to-ground lightning detection by a direction-finder network. *J. Geophys. Res.*, **94**, 13 313–13 318.
- , D. W. Burgess, V. Mazur, W. D. Rust, W. L. Taylor, and B. C. Johnson, 1989: Lightning rates relative to tornadic storm evolution on 22 May 1981. *J. Atmos. Sci.*, **46**, 221–250.
- Mach, D. M., D. R. MacGorman, W. D. Rust, and R. T. Arnold, 1986: Site errors and detection efficiency in a magnetic direction-finder network for locating lightning strikes to ground. *J. Atmos. Oceanic Technol.*, **3**, 67–74.
- Orville, R. E., R. A. Weisman, R. B. Pyle, R. W. Henderson, and R. E. Orville, Jr., 1987: Cloud-to-ground flash characteristics from June 1984 through May 1985. *J. Geophys. Res.*, **92**, 5640–5644.
- Reap, R. M., and D. R. MacGorman, 1989: Cloud-to-ground lightning: Climatological characteristics and relationships to model fields, radar observations, and severe local storms. *Mon. Wea. Rev.*, **117**, 518–535.
- Rust, W. D., D. R. MacGorman, and R. T. Arnold, 1981: Positive cloud-to-ground flashes in severe storms. *Geophys. Res. Lett.*, **8**, 791–794.
- , —, and S. J. Goodman, 1985: Unusual positive cloud-to-ground lightning in Oklahoma storms on 13 May 1983. Preprints, *14th Conf. Severe Local Storms*, Indianapolis, Amer. Meteor. Soc., 372–375.
- Schaefer, J. T., 1974: A simulative model of dryline motion. *J. Atmos. Sci.*, **31**, 956–974.
- Schlesinger, R. E., 1980: A three-dimensional numerical model of an isolated thunderstorm. Part II: Dynamics of updraft splitting and mesovortex couplet evolution. *J. Atmos. Sci.*, **37**, 395–420.
- Takagi, N., T. Takeuti, and T. Nakai, 1986: On the occurrence of positive ground flashes. *J. Geophys. Res.*, **91**, 9905–9909.
- Takeuti, T., M. Nakano, M. Brook, D. J. Raymond, and P. Krehbiel, 1978: The anomalous winter thunderstorms of the Hokuriku Coast. *J. Geophys. Res.*, **83**, 2385–2394.
- , Z.-I. Kawasaki, K. Funaki, N. Kitagawa, and J. Huse, 1985: On the thundercloud producing the positive ground flashes. *J. Meteor. Soc. Japan*, **63**, 354–357.
- U.S. Dept. of Commerce, 1984: *Storm Data*, **26**, No. 4, 50–51.
- Weisman, M. L., and J. B. Klemp, 1984: The structure and classification of numerically simulated convective storms in directionally varying wind shears. *Mon. Wea. Rev.*, **112**, 2479–2498.
- , and H. B. Bluestein, 1985: Dynamics of numerically simulated LP storms. Preprints, *14th Conf. Severe Local Storms*, Indianapolis, Amer. Meteor. Soc., 167–170.
- Wilhelmson, R. B., and J. B. Klemp, 1978: A numerical study of storm splitting that leads to long-lived storms. *J. Atmos. Sci.*, **35**, 1974–1986.
- Woodall, G. R., and H. B. Bluestein, 1988: Detailed observations of a splitting, “low precipitation” (LP) severe storm and its evolution into a supercell. Preprints, *15th Conf. Severe Local Storms*, Baltimore, Amer. Meteor. Soc., 280–283.